



Title	Computer Simulation of a Stress-Strain Curve with a Serrated Flow
Author(s)	Kimura, Yoshisato; Mohri, Tetsuo
Citation	北海道大學工學部研究報告, 155, 9-17
Issue Date	1991-05-24
Doc URL	<a href="http://hdl.handle.net/2115/42275">http://hdl.handle.net/2115/42275</a>
Type	bulletin (article)
File Information	155_9-18.pdf



[Instructions for use](#)

## Computer Simulation of a Stress-Strain Curve with a Serrated Flow

Yoshisato KIMURA\*\* and Tetsuo MOHRI\*  
(Received December 26, 1990)

### Abstract

A serrated plastic flow is observed on a stress-strain curve in almost all metallic materials. Computer simulation is proposed as one of helpful method for the study of such a serrated flow. As an initial basis of the simulation, calculation of the stress-strain curve for homogeneous deformation is performed. And by adding sinusoidal modulation to the average dislocation velocity of the homogeneous deformation, serrated flow on a stress-strain curve is obtained.

### 1. Introduction

In many cases, a serration occurs in a heterogeneous or a localized plastic deformation<sup>1,2)</sup>. Such a deformation causes a loss of efficiency of functional materials or a degradation of mechanical stability of structural materials. Thereby, it is deemed quite important to reveal the origin and general characteristic of the serration.

It is reported that a serration occurs in various manners depending on several factors, such as alloying elements, the shape of specimen, strain rates, temperatures, and so forth<sup>3)</sup>. To extract a general feature from the various experimental results and to synthesize several controlling factors, a theoretical investigation as well as an experimental study should be set forth. A computer simulation is regarded as a helpful method for a theoretical approach.

To the best of author's knowledge, a computer simulation for such a serration is attempted except for a study at cryogenic temperature performed by Shibata et al<sup>3)</sup>. They studied a particular case in which serration is caused by thermal instability due to the heat current generated by plastic deformation.

The primary aim of the present study is to generate a serrated stress-strain curve by modifying constitutive equations which have been employed to simulate an ordinary stress-strain curve for homogeneous deformation. Although the Portevin-Le Chatelier effect<sup>2,4,5)</sup> and propagations of deformation bands similar to Lüders band<sup>1,2)</sup> have been considered as the major mechanisms of a serration, no attempts have been made to synthesize a serrated stress-strain curve by explicitly taking into account above mechanisms into constitutive equations. Starting with the calculation for homogeneous deformation, we introduce the sinusoidal modulation into the mean dislocation velocity term and generate a stress-strain curve with

---

\* Department of Metallurgical Engineering, Hokkaido University, Sapporo 060 Japan

\*\* present adress ; Department of Materials Science, Tokyo Institute of Technology

a serration.

## 2. Theory for the calculation of a stress-strain curve

Two types of strain rate equations are conveniently defined for a specimen under a tensile test<sup>3,6)</sup>. One is an 'external' (or macroscopic) strain rate given by eq. (1) ;

$$\dot{\gamma}_{ext} = \frac{Sc - \frac{\dot{P}}{K}}{l_0 f_s} \quad (1)$$

where  $K$  is the stiffness of the testing system,  $Sc$  is crosshead speed and  $l_0$  is an initial length of a specimen,  $\dot{P}$  is a change of load during small time increment and  $f_s$  is a Schmid factor. Here, we assume that the specimen is subject to a plastic deformation only.

The other is an 'internal' (or microscopic) strain rate given by eq. (2) which is due to the movement of dislocations ;

$$\dot{\gamma}_{int} = N_m b \bar{v}, \quad (2)$$

where  $N_m$  is the mobile dislocation density,  $b$  is the Burgers vector and  $\bar{v}$  is the mean dislocation velocity.

Based on the assumption that the 'external' and the 'internal' strain rates are equivalent ( $\dot{\gamma}_{ext} = \dot{\gamma}_{int}$ ), the change in flow stress  $\tau$  during an infinitesimal displacement is represented by

$$\frac{d\tau}{dy} = \frac{K f_s}{A_0} \left( 1 - \frac{N_m b \bar{v} l_0 f_s}{Sc} \right) \quad (3)$$

Note that in order to obtain the equations above from eqs. (1) and (2), the following relations are employed ;

$$\frac{P}{A_0} = \frac{\tau}{f_s}, \quad (4)$$

and

$$Sc = \frac{dy}{dt}, \quad (5)$$

where  $y$  stands for the displacement of the crosshead which can be easily converted into strain and  $A_0$  is an initial cross sectional area of a specimen.

Among the parameters in eq. (3),  $N_m$  and  $\bar{v}$  sensitively depend on the microstructure. In the traditional Johnston-Gilman theory,  $N_m$  was simply assumed to increase monotonously in propotion to the square root of a strain  $\epsilon$ <sup>3)</sup>

$$N_m = N_0 + \alpha \epsilon^{\frac{1}{2}} \quad (6)$$

where  $N_0$  is an initial mobile dislocation density and  $\alpha$  is a multiplication rate. Although the eq. (6) may be rationalized for the initial stage of deformations, it is by no means acceptable that the  $N_m$  increases without an upper limit. In fact, Haasen and Alexander noticed this shortcoming and introduced the second constitutive relation which controls the mobile dislocation density<sup>6)</sup> ;

$$\frac{dN_m}{dy} = \frac{1}{Sc} \delta N_m \bar{v}, \quad (7)$$

where  $\delta$  represents a multiplication rate corresponding to  $\alpha$  in the eq. (6) and is given by

$$\delta = B\tau_{eff}, \quad (8)$$

where  $B$  is a constant specifying the degree of multiplication of dislocations and  $\tau_{eff}$  is an effective stress defined as

$$\begin{aligned} \tau_{eff} &= \tau_{app} - \tau_{in} \\ &= \tau_{app} - \frac{\mu b N_m^{\frac{1}{2}}}{\beta}. \end{aligned} \quad (9)$$

In the eq. (9),  $\tau_{app}$  and  $\tau_{in}$  are the applied stress and internal stress, respectively,  $\mu$  the shear modulus of a specimen and  $\beta$  is a parameter characterizing the interaction between dislocations<sup>6)</sup>. The entire idea of the condition devised by Haasen-Alexander is that the multiplied dislocations cause back stress field leading to the suppression of the further multiplications, which is virtually equivalent to the concept of work hardening.

In the present study, the conventional description for a mean dislocation velocity given by the eq. (10) is adopted<sup>2-4)</sup>.

$$\bar{v} = v_0 \exp\left(\frac{-U}{RT}\right), \quad (10)$$

where  $R$  and  $T$  are gas constant and absolute temperature, respectively,  $v_0$  the frequency factor and  $U$  stands for thermal activation energy for which the following Mott-Nabarro equation is employed<sup>7)</sup>.

$$\frac{U}{U_0} = \left\{1 - \left(\frac{\tau_{eff}}{\tau_0}\right)^2\right\}^{\frac{1}{2}} - \left(\frac{\tau_{eff}}{\tau_0}\right) \cos^{-1}\left(\frac{\tau_{eff}}{\tau_0}\right), \quad (11)$$

where  $U_0$  and  $\tau_0$  are constants.  $U_0$  corresponds to the energy needed to overcome an obstacle by thermal fluctuation and  $\tau_0$  means the stress required to move a dislocation at  $OK$ .

A stress-strain curve can be derived by solving simultaneous equations (3) and (7). As an initial condition, the followings are assumed;  $\tau_{eff}=0$  that is  $\tau_{app}=\tau_{in}$ , and  $N_m=N_0$  at  $y=0$  ( $\epsilon=0$ ). The parameters and constants used in the calculations are listed in Table. 1.

Table 1 The employed values of parameters and constants.

parameters and constants	values
b	$2.8635 \times 10^{-10}$ (m)
$\mu$	$2.7 \times 10^{10}$ (Pa)
$l_o$	0.02 (m)
$A_o$	$7.5 \times 10^{-6}$ (m)
$S_c$	$8.33 \times 10^{-6}$ (m/sec)
$N_o$	$10^8$ (m <sup>-2</sup> )
R	8.314 (J/K · mol)
$f_s$	0.4
$\beta$	3.3
$u_b$	$2.12 \times 10^{-7}$
$U_o$	$3.6 \times 10^4$ (J/mol)
K	10 (Pa · m)
B	$10^{-6}$

Table 2 The introduced dimensionless parameters.

dimensionless parameters	parameters and constants
S	$\frac{\tau}{\mu}$
N	$N_m b^2$
V	$\frac{v}{S_c}$
Y	$\frac{y}{b}$
$C_1$	$\frac{b}{\mu} \cdot \frac{K f_s}{A_o}$
$C_2$	$f_s \frac{l_o}{b}$
$C_3$	$b \mu B$
$C_4$	$\frac{u_b}{S_c}$
$C_5$	$\frac{U_o}{RT}$
$C_6$	$f_s$

Although the assignment of the material parameters should be carefully carried out to compare the results with the actual flow curve it is more convenient to scale the set of equations in order to discuss general feature of the flow curve rather than the characteristic aspects of each material. For this purpose, the dimensionless parameters are introduced and are listed in Table 2.

### 3. Simulations of a serrated flow

As was pointed out in the introduction section, the actual mechanism of serrated flow depends on various factors. The common feature, however, is considered to be the periodic variation of dislocation velocity as is exemplified in the following explanation for the Portevin-Le Chatelier effect in Fig. 1.

When solute atoms diffuse toward a dislocation in motion an atmosphere is formed to trap the dislocation, which raises the flow stress. The dislocation velocity, on the other hand, decreases gradually as the locking proceeds. At the stress level of a sufficiently large value that enables a dislocation to break away from atmosphere, the dislocation escapes and the velocity is accelerated. Accordingly, the flow stress is relaxed, which decelerates a dislocation velocity and solute atoms start diffusing to form an atmosphere again. Therefore, acceleration and deceleration of a dislocation velocity are considered to be key microscopic phenomena during a serrated flow. Based on this consideration, the periodic modulation is introduced to  $\bar{v}$  by imposing, for the simplicity, an arbitrary sinusoidal wave characterized by amplitude  $a$  and wave length  $c$ ,

$$\bar{v}_{sr} = \bar{v} + a \cdot \sin(c \cdot y), \quad (12)$$

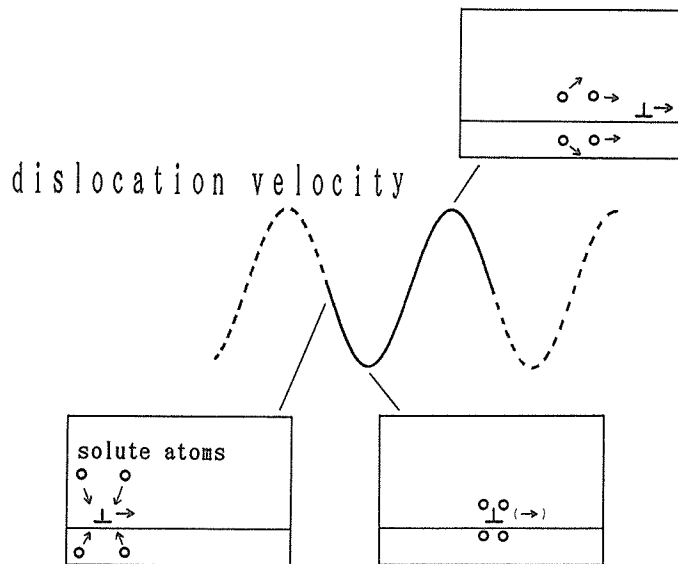


Fig. 1 Schematic illustration of Portevin-Le Chatelier effect and the variation of dislocation velocity.

where  $\bar{v}_s$  is the mean dislocation velocity with modulation.

## 4. Results and Discussions

### 4.1 Stress-strain curves for homogeneous deformations

An example of calculated stress-strain curve for 298K as well as the variation of mobile dislocation density, effective stress and mean dislocation velocity are demonstrated in Fig. 2. This curve is topologically quite similar to the one obtained from an actual tensile test. Although not shown here, the effect of raising temperature was investigated and it was confirmed that the entire level of flow stress decreases, which is exactly the case for an experimental observation.

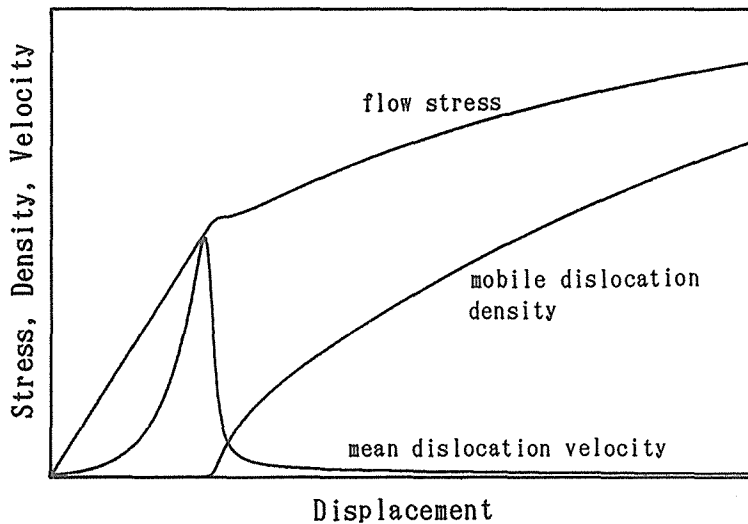


Fig. 2 An example of the calculated stress-strain curve for 298K with the variation of mobile dislocation density and mean dislocation velocity.

The yield point appears clearly on the stress-strain curve. It should be noted that even in the portion of the elastic deformation, plastic deformation takes place on a microscopic scale. In other words, elastic deformation of a specimen is not realized in this simulation. In the elastic region, flow stress increases monotonously being proportional to a strain, and  $\bar{v}$  begins to increase as the deformation proceeds. When  $\tau$  and  $\bar{v}$  reach certain values, plastic deformation commences on a macroscopic scale with the appearance of the yield point.

The topology of a calculated stress-strain curve which is characterized by the yielding behaviour and work hardening rates depends on the various parameters employed. Among them, the effect of the stiffness  $K$  of the testing system and multiplication rate  $\delta$  of mobile dislocations are investigated.

The effect of change in  $K$  is shown in fig. 3, where the assigned value of  $K$  is twice as large as that in Fig. 2. The slope of flow stress in the elastic range certainly increases. One should note that the degree of stress relaxation at the yielding point is emphasized. This

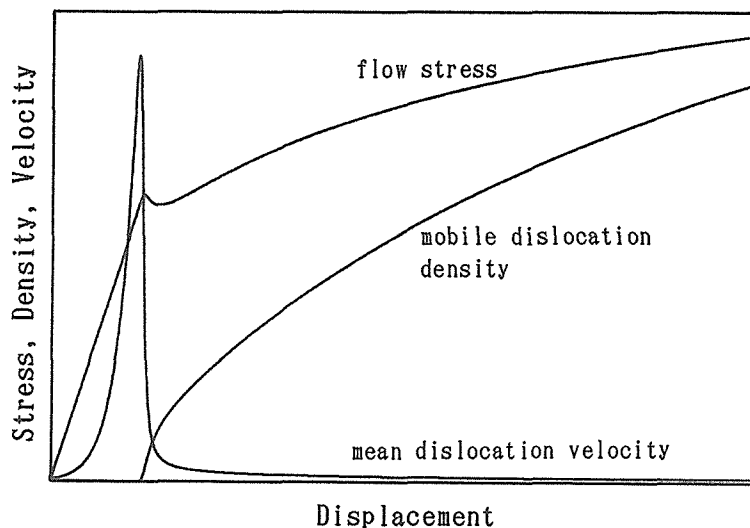


Fig. 3 The effect of change in the value of  $K$  on a calculated stress-strain curve for 298K. The assigned value of  $K$  is twice as large as that in Fig. 2.

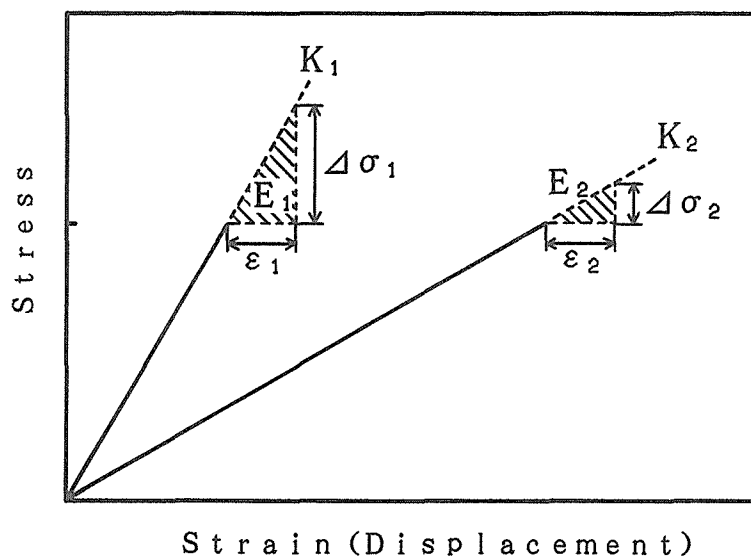


Fig. 4 The dependence of elastic energy per unit strain on the difference of the stiffness of the testing system. The hatched area represents elastic energy per unit strain. The elastic energy  $E_i$  as well as  $\Delta\sigma_i$  are greater for  $i=1$  than 2 when  $K_1 > K_2$  and  $\epsilon_1 = \epsilon_2$ .

may be due to the reason that the elastic energy per unit strain which is expected to be released is larger for larger  $K$  value as schematically indicated in Fig. 4. It is also noted that the work hardening rate does not have a dependency on the value of  $K$  after yielding.

The effect of change in  $\delta$  (or  $B$ ) is shown in Fig. 5, where the assigned value of  $\delta$  is twice as large as that in Fig. 2.  $N_m$  and the multiplication rate increase apparently with the value of  $\delta$ , while  $\bar{v}$  decreases reciprocally proportional to  $N_m$ , which suggest that the density and mobility of dislocations are inversely proportional each other under the constant internal strain rate. One should also note that the yield point is now less pronounced and work hardening rate becomes larger.

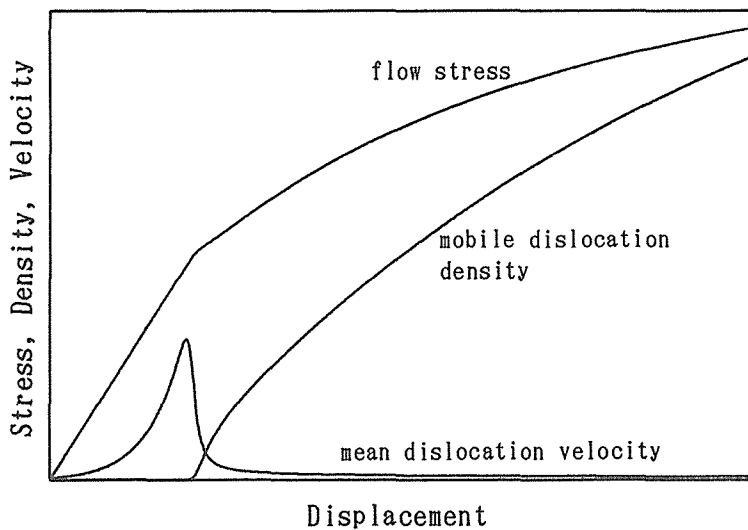


Fig. 5 The effect of change in the value of  $\delta$  on a calculated stress-strain curve for 298K. The assigned value of  $\delta$  is twice as large as that in Fig. 2.

#### 4.2 Stress-strain curves with serrations

As an initial attempt to simulate a serrated flow, a sine wave modulation is imposed as is shown in eq. (12). Fig. 6 shows an example of the calculated results. The values of parameters and constants employed here are the same ones listed in Table. 1. In addition,  $2 \times 10^{-8}$  and 0.2, respectively, are assigned to  $a$  and  $c$ .

One can see that the modulation of  $\bar{v}$  are reflected on flow curve as a serration. Also a modulation is induced to  $N_m$  as well. It is noted that the amplitude of the serration increases with the displacement in spite of the fact that a modulation amplitude imposed on  $\bar{v}$  is a constant value. Such a tendency of an amplification of the serration is actually observed in a real serrated flow curve<sup>8)</sup>.

The serration behaviour has been regarded as a cyclic repetition of a yielding behaviour. Hence a similar response to the change in  $K$  and  $\delta$  can be expected. In fact, one can see in Fig. 7 that the increment of  $K$  induces the amplification of the serration. Similar behaviour



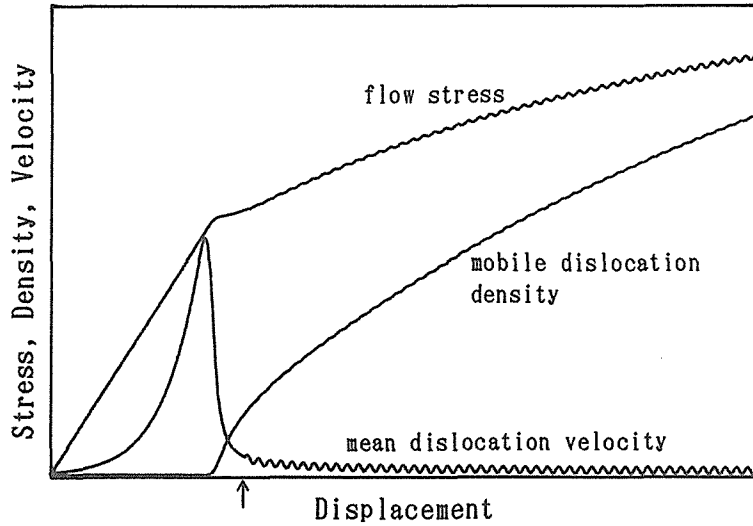


Fig. 6 An example of the calculated serrated stress-strain curve for 298K. The imposition of the modulation on  $\bar{v}$  is started at the displacement shown by an arrow.

is also confirmed for the decrease of  $\delta$ .

The response of the serration is not linear mathematically, and the amplitude seems to increase unboundedly. In order to simulate a more complicated serration behaviour by adding other sine wave spectrum, the suppression mechanism of the amplification should be clarified, which remains for further work.

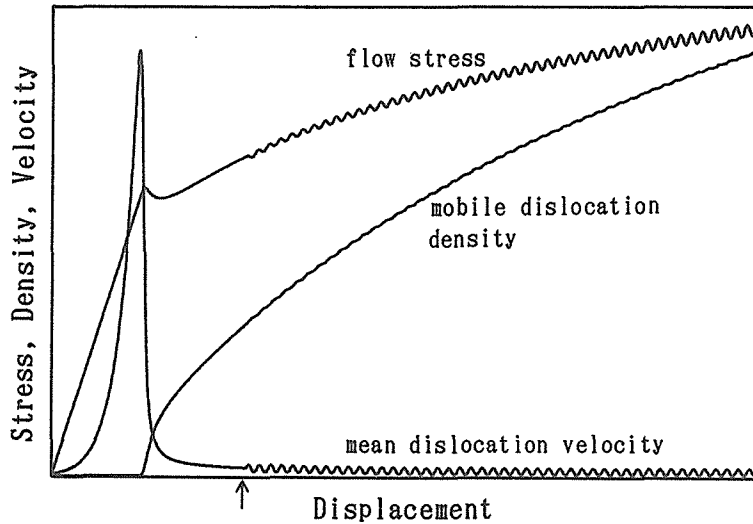


Fig. 7 The effect of change in the value of  $K$  on a calculated serrated stress-strain curve for 298K. The assigned value of  $K$  is twice as large as that in Fig. 6.

## 5. Summary

A sinusoidal modulation was imposed on the average dislocation velocity of the constitutive equations which describe a homogeneous deformation. Based on the new set of constitutive equations, the stress-strain curve is calculated and the serrated flow curve is successfully reproduced. The amplitude of the serration is amplified with the strain, which is the case observed in the experiment.

## Acknowledgement

The authors are grateful for the stimulating discussions with Mr. Hisa.

## References

- 1) H. Fujita and T. Tabata : *Acta metall.*, 25 (1977), pp. 793-800
- 2) A. Pawelek : *Z. Metallkde*, 80 (1989), pp. 614-618
- 3) K. Shibata and T. Fujita : *Trans. ISIJ*, 26 (1986), pp. 1065-1072
- 4) P. G. McCormick : *Acta metall.*, 19 (1971), pp. 463-471
- 5) E. Pink and A. Grinberg : *Acta metall.*, 30 (1982), pp. 2153-2160
- 6) M. Suezawa, K. Sumino, and I. Yonenaga : *phys. stat. sol.*, (a) 51 (1979), pp. 217-226
- 7) H. Suzuki : *Teniron. nyumon*, (1989), pp. 297-308
- 8) K. T. Hong and S. W. Nam : *Acta metall.*, 37 (1989), pp. 31-34